Solvent-Dependent Photoinduced Tautomerization of 2-(2‘-Hydroxyphenyl)benzoxazole

ARTICLE *in* THE JOURNAL OF PHYSICAL CHEMISTRY A · MARCH 2002

Impact Factor: 2.69 · DOI: 10.1021/jp013915o

5 AUTHORS, INCLUDING:

Osama Kamal Abou-Zied
Sultan Qaboos University
50 PUBLICATIONS **947** CITATIONS
SEE PROFILE

Ralph Jimenez
University of Colorado Boulder
89 PUBLICATIONS **3,386** CITATIONS
SEE PROFILE

David P Millar
The Scripps Research Institute
108 PUBLICATIONS **3,536** CITATIONS
SEE PROFILE

Solvent-Dependent Photoinduced Tautomerization of 2-(2′-Hydroxyphenyl)benzoxazole

Osama K. Abou-Zied,[†] Ralph Jimenez,[†] Elizabeth H. Z. Thompson,[‡] David P. Millar,[‡] and Floyd E. Romesberg*,[†]

Departments of Chemistry and Molecular Biology, The Scripps Research Institute, 10550 N. Torrey Pines Rd., Maildrop CVN22, La Jolla, California 92037

Received: October 22, 2001; In Final Form: January 22, 2002

The solvent-dependent ground-state conformational equilibrium and excited-state dynamics of 2-(2′-hydroxyphenyl)benzoxazole have been characterized in several solvents on the femtosecond to nanosecond time scales. The only observable ground-state tautomer is the enol, which exists in equilibrium between the *syn*- and *anti*-rotational isomers. In the *anti*-enol isomer, the phenyl hydroxyl group appears to not interact strongly with solvent but rather forms a strong intramolecular hydrogen bond with the benzoxazole oxygen atom. In the *syn*-enol isomer, the phenyl hydroxyl proton may interact with solvent or form an internal hydrogen bond with the benzoxazole nitrogen atom. Upon excitation, the proton is transferred from the oxygen atom to the nitrogen atom of the internally hydrogen bonded *syn*-enol isomer in 170 fs, regardless of the solvent. The lifetime of the resulting excited keto tautomer is solvent dependent and on the order of picoseconds. In addition to these dynamics, several additional dynamic processes are detected which may correspond to relaxation of a distorted excited keto tautomer.

Introduction

Proton-transfer reactions are of fundamental importance in chemistry and biology. A variety of molecules have intramolecular hydrogen bonds (H-bonds) that may be photoinduced to undergo proton transfer.[1,2] This process is known as excited-state intramolecular proton transfer, or ESIPT. Molecules that can undergo ESIPT allow for the controlled initiation and subsequent time-dependent characterization of both the H-bond itself and the proton transfer process. We have recently proposed one such molecule, 2-(2′-hydroxyphenyl)benzoxazole (HBO), as a structural mimic of a DNA base pair for which tautomerization may be initiated at a defined time and position within duplex DNA (Figure 1).[3] In contrast to previous model base pairs, such as dimers of 7-azaindole,[4] HBO may be incorporated into duplex DNA.[3] Therefore, HBO may be used to probe the biologically relevant duplex environment. Experimental (UV/vis, CD, duplex melting temperature) and theoretical studies (molecular dynamics simulations) of DNA containing the HBO model base pair demonstrate that, in a given DNA sequence context, HBO packs within an A-form duplex and that the resulting duplex has a structure and stability similar to a fully native duplex. The conformational and tautomerization dynamics of the model base pair are dominated by interbase packing effects that are unique to the duplex environment.[5] To fully interpret the effects of the biological environment on the dynamics of the HBO model base pair it is important to understand the dynamics of HBO in a variety of simple solvent environments.

Several studies have documented the solvent-dependent conformational isomerism of HBO and several analogues, including 2-(2′-hydroxyphenyl)benzothiazole (HBT), 2-(2′-hydroxyphenyl)benzimidazole (HBI), and 2-(2′-hydroxyphenyl)-4-methyloxazole (HPMO).[6−17] In the ground state, HBO, HBT, HPI, and HPMO exist in a conformational equilibrium between the *syn*- and *anti*-enols. In addition, the phenoxy group of each *syn*-enol may form an internal H-bond or an intermolecular H-bond with a solvent molecule (referred to as "solvated" or "open"). Only the internally H-bonded *syn*-enol efficiently forms the keto tautomer due to favorable electronic (ΔpK_a) and structural properties (H-bond). Proton transfer does not occur in the *anti*-enol species due to an insufficient increase in the basicity of

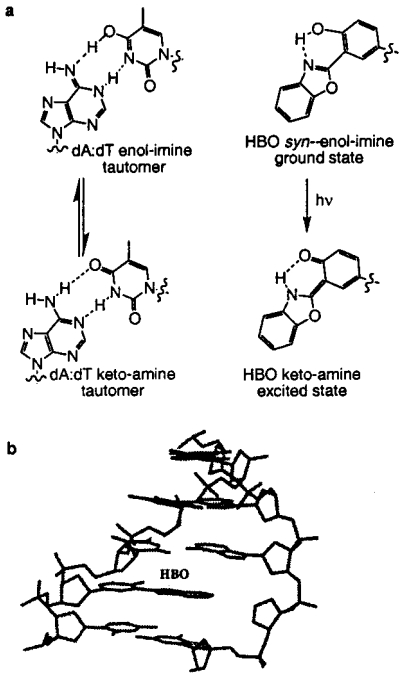

Figure 1. (a) Tautomerization of a natural DNA base pair and ESIPT in HBO. (b) Modeled structure of DNA duplex containing an HBO model base pair.[3,5]

* Corresponding author. E-mail: floyd@scripps.edu. Fax: (858) 784 7472.
[†] Department of Chemistry.
[‡] Department of Molecular Biology.

10.1021/jp013915o CCC: $22.00
Published on Web 03/26/2002

the oxygen, sulfur, and secondary amine groups in HBO, HBT, and HBI, respectively, upon excitation. In the *syn*-enol ESIPT results in diminished fluorescence in the normal Stokes-shifted emission region, ascribable to the excited enol, and instead fluorescence is observed at longer wavelengths, due to the excited keto (ESIPT product). In non-H-bonding solvents, such as hexane, which are unable to effectively compete for the phenolic proton, excitation results in very efficient ESIPT and long-wavelength fluorescence. However, in protic solvents, which are more able to compete for the phenolic proton, emission from both enol and keto are observed with intensities that depend on the concentration of the *syn*-enol relative to the solvated and *anti*-enols.

Several time-resolved studies have characterized the HBO proton-transfer dynamics and the lifetime of the enol and keto tautomer excited states. The short wavelength fluorescence of HBO was reported to have a decay time constant of 1080 ± 360 ps in dimethyl sulfoxide (DMSO)[8] In HBI, the excited-state lifetime for the *anti*-enol species is reported in neutral aqueous and ethanol solutions to be 370 ps and 1.5 ns, respectively.[9,10] Most of the published work on HBO has only been able to assign an upper limit (~10 ps) to the ESIPT time constant.[8] With femtosecond time resolution, Ernsting and co-workers measured a gain in the transient absorption signal of 60 ± 30 fs, which was assigned to keto tautomer formation in the excited state.[11] However, the pulse duration used in the experiment (170 fs) indicates that the measured time constant for the HBO ESIPT process may not be accurate. Laermer and co-workers measured an HBT ESIPT time constant in tetrachloroethylene of 170 ± 20 fs.[12] The ESIPT reaction has also been observed for HBT in polar solvents, but the proton-transfer kinetics do not show simple monoexponential behavior, although they do occur on a similar time scale as that observed in tetrachloroethylene.[13] Only an upper limit of 100 ps has been determined for the proton-transfer time constant in HBI due to insufficient time resolution.[10] HPMO ESIPT is thought to proceed by two distinct mechanisms.[14] The first, a direct proton transfer, was characterized by a 100 fs time constant, while the second pathway involved twisting motion of the biaryl ring system and was characterized by two time constants of 200 fs and 3 ps. The HBO keto lifetime was found to be solvent dependent, displaying an apparent inverse relationship with the solvent dielectric constant and ranging from ~70 to ~ 400 ps.[15] The lifetime of the keto tautomer of HBT in solution at room temperature lies in the subnanosecond range.[16−18] The decay profile is biexponential and wavelength-dependent either as a result of vibrational relaxation processes or due to emission from both *syn*- and *anti*-keto species. In HBI, fluorescence lifetime for the keto species is reported in neutral aqueous and ethanol solutions to be 1.8 and 4.1 ns, respectively.[9,10] With HPMO, the planar excited-state ketone was found to have a 2−6 ps lifetime in *p*-dioxane.[14]

No comprehensive characterization of conformation equilibrium and excited-state dynamics of HBO has been reported. Therefore, to develop a more thorough understanding of the environmental factors effecting the tautomerization of HBO, a steady-state and time-resolved characterization of HBO was carried out in solvents of differing polarities and H-bonding abilities. Three solvents were chosen, hexane, in which virtually only low-energy keto HBO fluorescence is detected, methanol (MeOH), where enol and keto fluorescence are both detected, and DMSO, in which most of the detected fluorescence is from the enol species. Femtosecond one-color and two-color transient absorption (TA) pump−probe experiments, as well as picosecond time-resolved fluorescence (TRF) spectroscopy, were employed to access the wide range of time scales required to follow all of the ESIPT dynamics and assign the molecular origin of each signal.

Materials and Methods

Sample Preparation and Characterization. HBO was purchased from Aldrich and purified by vacuum sublimation. 2-(4-Biphenylyl)-6-phenylbenzoxazotetrasulfonic acid potassium salt (furan-2) was purchased from Lambda Physik. MBO was synthesized by dissolving HBO in *N*,*N*-dimethylformamide (DMF) and adding a slight excess of K_2CO_3 and methyl iodide and purified by column chromotography. HPLC grade hexane and methanol (Fischer Scientific) and DMSO (Aldrich) were used without further purification.

Steady-State Absorption and Fluorescence. Steady-state absorption spectra were measured using a Cary 300 BIO spectrophotometer. Samples were contained in a 1 cm path length quartz cell containing approximately 50 μM solutions, and fluorescence spectra were measured on Spex Fluorolog spectrometer in 1 cm path length quartz cell using a right angle detection configuration.

Transient Absorption (TA). The transient absorption measurements were performed using a pump−probe setup. A home-built, diode laser (Spectra Physics Millenia) pumped, mode-locked, titanium:sapphire oscillator produces sub-30-fs pulses centered at 800 nm. The pulses are amplified by a commercial chirped pulse amplifier system (Spectra Physics Spitfire/Evolution). The amplifier produces 40−50 fs pulses centered at 800 nm at a 1−5 kHz repetition rate. Frequency conversion is accomplished with a home-built optical parametric amplifier (OPA) and is based on the design of Yakovlev et al.[19] The signal beam from the OPA is subsequently doubled twice in two type I BBO crystals to generate approximately 10−20 μJ energy in the UV region (300−340 nm). The pulses are compressed by double passing through a pair of fused silica prisms to compensate for the group velocity dispersion.

In the one-color TA experiments, the pulses were split into a pump pulse (2/3) and a probe pulse (1/3). The pump pulse traveled a constant distance to the sample cell while the probe pulse was delayed in time before being directed into the cell. In the two-color TA experiments, light from the idler beam of the OPA was doubled twice to obtain a probe pulse with a wavelength in the blue region (420−460 nm). A beam splitter was used to split a small portion of the probe beam to be used as a reference beam. The excitation, probe, and reference beams were focused into the sample with a fused silica lens ($f \approx 10$ cm), but only the excitation and signal beams were overlapped in the sample. The sample was contained in a 0.2 mm quartz flow cell. After passing through the sample, both signal and reference beams were detected using silicon photodiodes. The signal levels were recorded by lock-in amplifiers referenced to a phase-locked chopper (synchronized to the amplifier Q-switch), which blocks half the pulses in the excitation beam. The delay stage and data acquisition were controlled with a PC. It was typically possible to measure samples with optical density on the order of 10^{-4}, after averaging the signal from ~5000 pulses for each delay position. All experiments were carried out at room temperature. The finite response time of the system was determined by recording the absorption change of furan-2 in water. The data were fit by numerical iterative convolution using a variable Gaussian instrument response function to obtain the best fit with the observed decay, as judged by the distribution of weighted residuals. The calculated full-width at half-

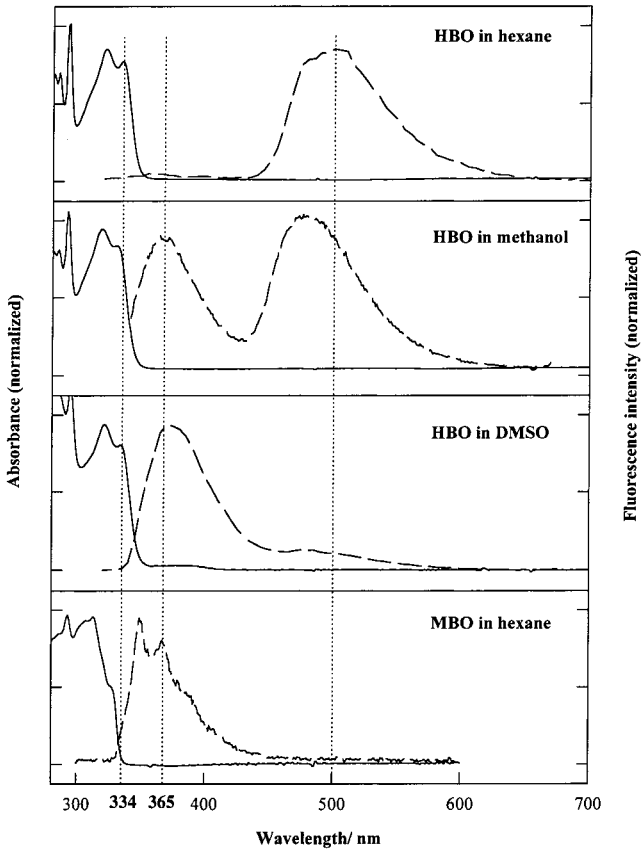

Figure 2. Absorption (solid lines) and emission (dashed lines) spectra of HBO dissolved in hexane, methanol, and DMSO. The spectra of MBO dissolved in hexane is also shown. The excitation wavelength was 320 nm.

maximum (fwhm) was ~89 fs in both the one- and two-color experiments. The fit also serves to locate time zero. Due to the use of a single OPA, a change in the pump wavelength required a change in the probe wavelength. Therefore, to examine the wavelength dependence of the TA signals, three two-color experiments were conducted with pump/probe wavelengths of 320/430, 333/445, and 338/453 nm.

Time-Resolved Fluorescence (TRF). The time-dependent emission was measured using time-correlated single photon counting which has been described elsewhere.[20] Briefly, samples contained in quartz cells (1 cm path length) were excited at 333 nm using the frequency-doubled output from a synchronously pumped, mode-locked, and cavity-dumped dye laser (Coherent 702). Sample emission was collected at right angles to the excitation beam, collimated by a lens, passed through a motor-controlled polarizer, and focused on the entrance slit of a monochromator (Jobin-Yvon H-10). Emission at 362−370 and 480−500 nm was examined. The instrument response function of the system was obtained by recording the scatter of the second harmonic of the excitation pulse and determined to have a width of 100 ps (fwhm).

Results

Absorption and Fluorescence Steady-State Spectra. To characterize the effects of solvation on the steady-state spectroscopic properties of HBO, the absorption and emission spectra were recorded in hexane, MeOH, and DMSO (Figure 2). Features in the absorption spectra of HBO have previously been assigned by Dörr et al. on the basis of a comparison with model compounds where H-bonding is not possible, as well as ^{1}H NMR

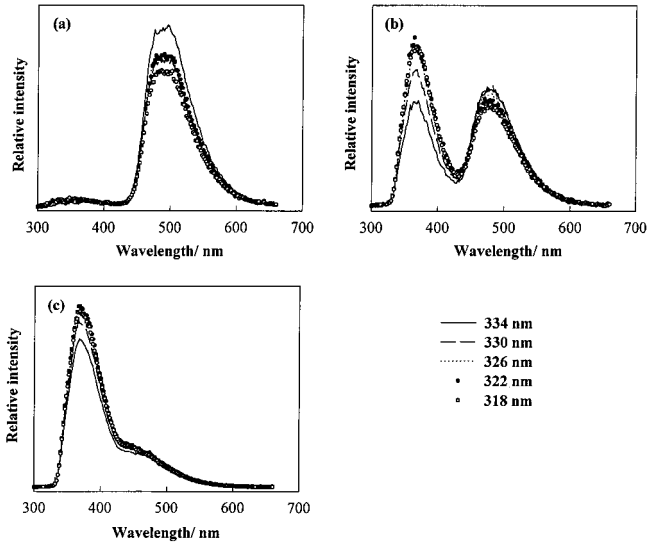

Figure 3. Steady-state emission spectra of HBO in (a) hexane, (b) methanol, and (c) DMSO. The spectra were measured at different excitation wavelengths as indicated in the figure and the text.

and IR spectroscopy.[8] The presence of an HBO anion is excluded on the basis of the work of Krishnamurthy and Dogra[7] as well as Mosquera et al.[10] HBO shows two, low-energy $\pi\pi^*$ absorptions. Following the assignments of Dörr et al., an absorption at ca. 320 nm is assigned to the *anti*-enol and an absorption at ca. 330−334 nm corresponds to the *syn*-enol.[8] Both transitions are at the same wavelength in hexane and DMSO (321 and 334 nm) but slightly blue-shifted in methanol (319 and 330 nm). This result is not consistent with simple polarity effects and may derive from specific H-bonding between the methanol donor and either the benzoxazole nitrogen or oxygen acceptors. A weak absorption band at ~370 nm was observed in DMSO. This absorption was assigned by Dörr et al. to the *anti*-keto tautomer. The fluorescence spectrum consists of two strong emission bands at ca. 362−370 nm and 474−500 nm, whose peak frequencies and relative intensities are solvent dependent. The UV emission arises from the enol tautomer, while the lower energy emission arises from the keto tautomer after ultrafast ESIPT from the initially prepared enol tautomer. These assignments are supported by absence of the low-energy emission band in the fluorescence spectrum of 2-(2′-methoxyphenyl)benzoxazole (MBO, Figure 2), which, due to the methoxy group, serves as a non-proton-transfer model. The keto emission band is dominant in hexane (at 500 nm), keto and enol (at 365 nm) emission bands are of equal intensity in methanol, and the enol emission band is dominant in DMSO. The enol emission spectrum is shifted to lower energy in methanol and DMSO (365 and 370 nm, respectively) relative to that in hexane (362 nm). The opposite trend is observed for keto emission where the emission wavelength is shifted to higher energy in methanol and DMSO (474 and 463 nm, respectively) relative to that in hexane (500 nm).

Fluorescence emission spectra measured at various excitation wavelengths in different solvents (Figure 3) revealed the relative concentrations of the solvated *syn*- and *anti*-enols that contribute to the emission band at 362−370 nm. In hexane, fluorescence in this region is negligible after excitation in the 333 nm region (*syn*-enol λ_{max}), while fluorescence at these wavelengths is maximal following excitation at 318 nm (*anti*-enol λ_{max}). Therefore, we assign the majority of HBO emission in hexane in this region to fluorescence of the excited anti-conformer. In methanol and DMSO, the fluorescence emission spectra mea-

TABLE 1: Time Constants (ps) Measured by TA and TRF[a] and Their Assignments

solvent	$\lambda_{detection}$, nm	solvated enol	*anti*-enol	τ_n[b]	keto
			Transient Absorption		
hexane				12 (0.50)[c]	295 (0.50)
				20 (0.12)[d]	295 (0.88)
				0.56 (rise)[e,f]	295
methanol				12 (0.67)[c]	68 (0.33)
				0.56 (rise)[e]	68
DMSO				12 (0.15)[c]	57 (0.85)
				0.56 (rise)[e]	57
			Time-Resolved Fluorescence		
hexane	362		1370 (0.50)		295 (0.50)
	500				295
methanol	365	510 (0.64)	1560 (0.36)		
	474		1560 (<1%)		68[g] (>99%)
DMSO	370	970 (0.35)[h]	1380 (0.65)[h]		
	463		1380 (<1%)		57[g] (>99%)

[a] Unless noted, time constants represent decays. Relative contributions are listed in parentheses. [b] Unassigned intermediate time scale dynamics. See text for details. [c] One-color TA (333/333 nm). [d] Two-color TA (320/430 nm). [e] Two-color TA (333/445 nm). [f] Two-color TA (338/453 nm). [g] Fit based on TA data. [h] See text for assignment.

sured at various excitation wavelengths showed a considerable contribution from the excited states of both solvated *syn*- and *anti*-conformers to the emission in this region. Therefore, relative to hexane, MeOH and DMSO increase the stability of the solvated *syn*-enol relative to the *anti*-enol of HBO, presumably due to stronger H-bonding between the solvent and the HBO hydroxyl group in the *syn* conformation.

The methoxy derivative of HBO (MBO) shows absorption maxima in hexane (313 and 324 nm) that are slightly blue-shifted relative to those of HBO (Figure 2), which may result from steric effects induced by the larger methoxy group of MBO relative to the smaller hydroxy group of HBO. The larger methoxy group may interfere with coplanarity of the two aromatic rings and results in reduced delocalization of electron density through the conjugated biaryl system. The emission of MBO is more structured and blue-shifted relative to HBO. The nearly mirror image relationship to the absorption spectrum is consistent with the absence of ESIPT-mediated relaxation in the excited state.

Time-Resolved Absorption and Fluorescence. Time-resolved experiments were performed to characterize the dynamics of HBO in each solvent (Table 1). One- and two-color TA was employed to measure the fast dynamics (100 fs to 300 ps), and TRF was used to measure slower decays (100 ps to 20 ns). The one-color TA experiments may be complicated by probe pulse (333 nm) absorption in either enol or keto excited states in addition to ground-state absorption. Two-color TA experiments were performed with pump/probe wavelngths of 320/430, 333/445, and 338/453 nm to examine the wavelength dependence. The TRF detection wavelength was chosen on the basis of the steady-state emission maxima, described above, to probe specific emitting species. The average lifetime values are reported for cases where the same decay component was measured with both methods or for cases where the component was detected at two different fluorescence detection wavelengths.

Transient Absorption Spectroscopy. The TA data for HBO in hexane are shown in Figures 4, 5, and 6a. The small decrease in intensity around zero delay may be due to absorption from the S_1 state of the enol, as suggested previously.[21] The data from the one- and two-color experiments are collected in Table 1. The fastest time scale dynamics are illustrated for the two-color experiment (333/445 nm) in Figure 4. For comparison, the presumably response limited rise time of furan-2 is also shown. The pump pulse prepares the system in the enol excited state, from which the *syn*-tautomer promptly tautomerizes by ESIPT to the keto tautomer. The fast time scale dynamics of HBO lead to a signal rise after time zero as shown in Figure 4, which reflects proton transfer. The rise time is apparent and identical in each experiment. The rise time is attributed to absorption of the excited-state keto. The data are fit with a single

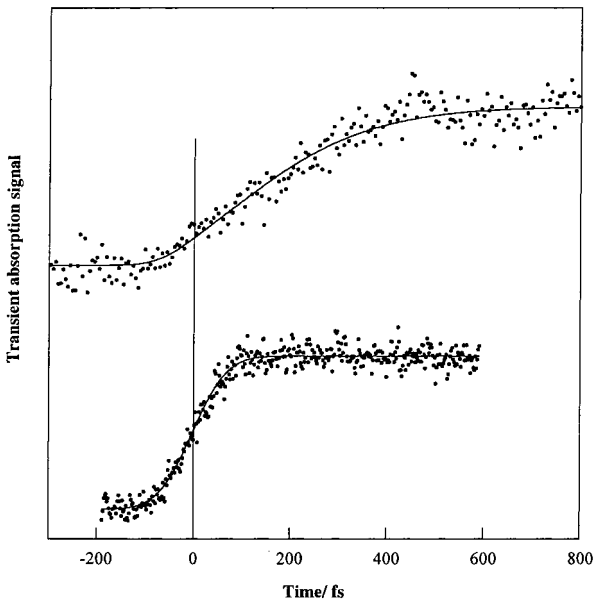

Figure 4. Femtosecond transient absorption of HBO in hexane (top) and furan-2 in water (bottom). Excitation and probe wavelengths were 333 and 445 nm, respectively. The data are plotted as a function of the delay time between pump and probe pulses. The rise in furan-2 reflects the time-integrated cross-correlation function of the two pulses. The rise time onset of the signal in HBO reveals the formation of the keto species by ESIPT. The solid lines represent the best fits from a rate equation model as explained in the text.

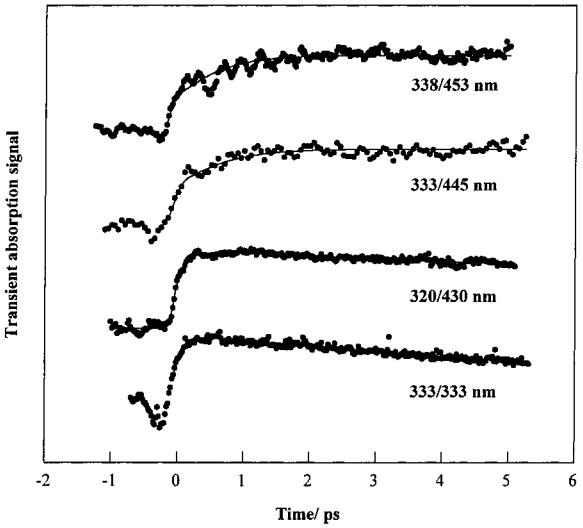

Figure 5. Femtosecond transient absorption of HBO in hexane in the intermediate time frame from 0 to 5 ps. Pump−probe wavelengths employed are indicated in each case. The solid lines are the best fits. The analysis gives a rise time of 170 fs in all the transients followed by a decay of 12 ps in the one-color experiment, a decay of 20 ps in the 320/430 nm two-color experiment, and a rise time of 560 fs in the 333/345 and 338/453 nm experiments. The fit is calculated from time origin in the case where an absorption decrease around zero delay is observed.

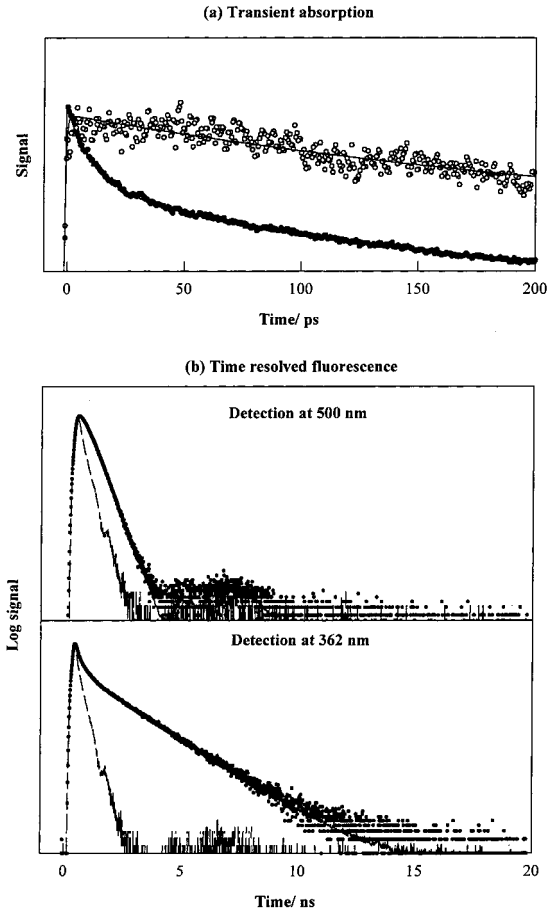

Figure 6. Time-resolved (a) transient absorption and (b) fluorescence of HBO in hexane (0−20 ns). Transient absorption is shown for the one-color experiment (closed circles) and the 333/445 nm two-color experiment (open circles). The excitation wavelength in the TRF experiment was 333 nm, and the detection wavelength is shown for each case. The data from the TRF experiment were fit to a biexponential decay convoluted with the instrument response function shown in the figure as a dashed line.

rise exponential function convoluted with an 89 fs pulse width. A time constant for the proton transfer of 170 ± 20 fs was determined. This conclusion is confirmed by measuring the TA of MBO, which is incapable of tautomerization and shows no rise time (Figure 7). This time constant may not directly represent the ESIPT rate constant. The use of a time constant determined from monitoring a single wavelength requires two assumptions. The transition moment must be wavelength independent (Condon approximation), and the time constant must not reflect vibrational relaxation within the product manifold. It is unclear to what extent these approximations are justified in this study. Nevertheless, it is clear by comparison with MBO that the 170 fs time scale is associated with the proton transfer and, therefore, represents an upper limit to the transfer time. Within experimental error, the same time constant was observed in MeOH, MeOD, and DMSO, indicating that the proton transfer is solvent and isotope independent. These results agree with those obtained previously for the thiazole analogue HBT.[12,13]

The TA experiments also exhibited a 0.5−20 ps time scale process. The observed process was strongly dependent upon the pump and probe wavelengths (Figure 5). The single color data (333/333 nm) showed a decay with a time constant of 12 ps, while the two-color data (320/430 nm) showed a similar decay with a slower time constant of 20 ps. However, a rise

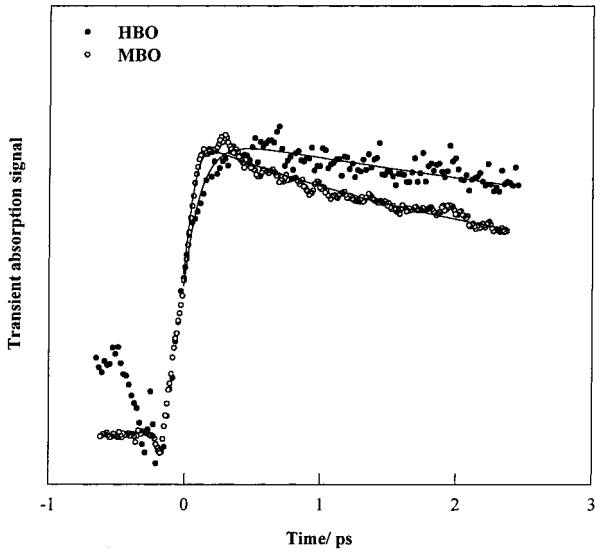

Figure 7. Single-color (333 nm) femtosecond transient absorption of HBO and MBO in hexane. Solid lines represent the best fit to the data calculated from time zero.

time of 560 fs was observed in the 333/445 and 338/453 nm TA data. The one-color (333/333 nm) and the two-color (333/445 nm) experiments were also performed with HBO in MeOH and DMSO, which showed identical time constants (a 12 ps decay and a 560 fs rise, for the one- and two-color experiments, respectively). The molecular origin(s) of this intermediate time scale decay or rise component is unclear (vide infra). Oscillations which persist for at least 5 ps are observed in almost all of the transients (Figure 5). These oscillations may be due to a vibronic wave packet that is created in the keto S_1 state after ESIPT. However, the presence of such oscillations in MBO indicates that this wave packet motion may be associated with vibrational modes in the S_0 or S_1 state of the enol tautomer.

HBO also possesses longer time scale dynamics in hexane. A 295 ps decay is observed in the one- and two-color (333/445, 320/430 nm) TA experiments. This time constant is consistent with that observed in cyclohexane for the excited-state keto lifetime (257 ps).[15] The observed 295 ps decay is therefore assigned to excited-state keto lifetime. One color and two-color (333/445 nm) TA data for HBO in MeOH and DMSO showed a 68 and 57 ps decays, respectively, again assigned to the keto excited-state lifetime, in agreement with previous studies.[8,15]

Time-Resolved Fluorescence Studies. The TRF transients of HBO in hexane monitored in either the enol emission region (362 nm) or keto emission region (500 nm) are shown in Figure 6b. With 362 nm detection, a biexponential decay was observed with short and long components of 295 and 1370 ps, respectively. The 295 ps decay matches the TA decay and is assigned to the excited keto lifetime (detected in the very blue edge of the emission band), and the 1370 ps decay is assigned to lifetime of the excited *anti*-enol, based on the excitation dependent study described above. With detection at 500 nm, only a 295 ps decay was observed, which is consistent with excited keto emission.

The TRF of HBO in methanol was monitored at either 365 or 474 nm. At 365 nm, two decays were apparent with time constants of 510 and 1560 ps, corresponding to the two enol conformers, as shown in the excitation-dependent experiments described above. The 1560 ps decay may be assigned to the excited *anti*-enol lifetime on the basis of the similarity to the long time scale observed in hexane. By elimination, the 510 ps

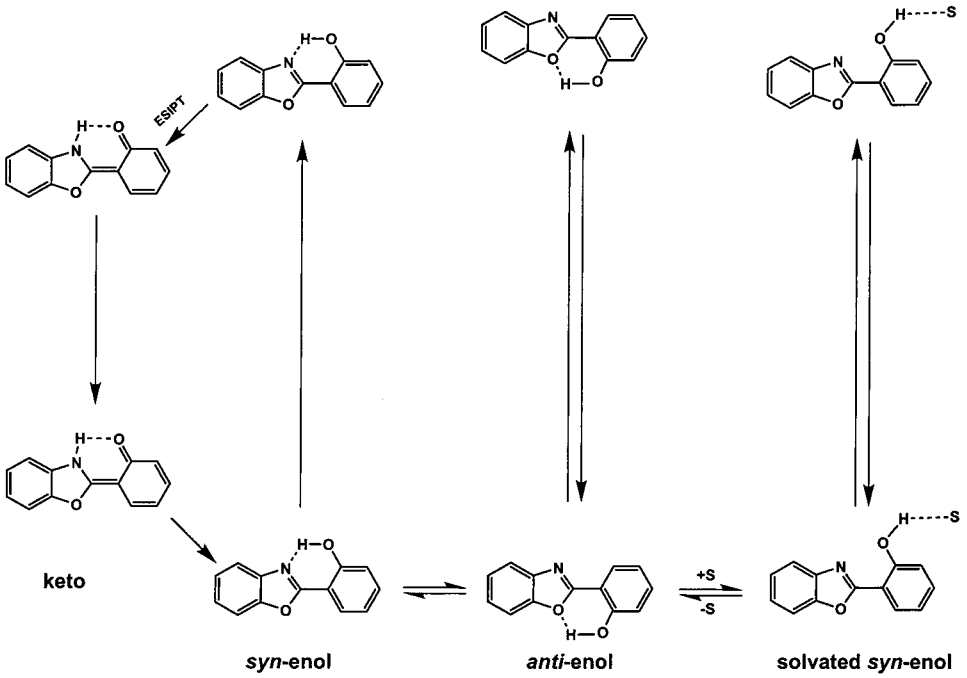

Figure 8. Ground-state equilibria and excited-state dynamics of HBO.

decay is assigned to the solvated *syn*-enol excited state. With 474 nm detection an instrument-limited decay was detected that must correspond to the decay of the keto excited state (measured above to be 68 ps). A small amplitude component (<1%) of the 1560 ps decay was also present due to detection of the low-energy tail of the *anti*-enol fluorescence.

The TRF of HBO in DMSO was monitored at either 370 or 463 nm. At 370 nm, two decays were apparent with time constants of 970 and 1380 ps. The difference between these time constants is not as large as those in MeOH, and therefore, their assignment is more difficult. In analogy to the experiments described above, the 970 and 1380 ps decays may be assigned to the solvated *syn*- and *anti*-enols, respectively. However, we note that the relative amplitudes of the two decays are more consistent with the opposite assignments considering excitation at 333 nm (maxima of the *syn*-enol absorption). With 463 nm detection a pulse limited decay was also detected and is assigned to keto excited state (on the basis of the TA experiments described above, the lifetime is 57 ps). As with methanol, a small contribution (<1%) from the *anti*-enol fluorescence decay was detected at 463 nm. The assignments of the two enol lifetimes are consistent with previous studies.[8,15]

Discussion

Solvent-Dependent Conformational Equilibrium of HBO. The solvent-dependent conformational equilibrium of HBO is depicted in Figure 8. Two rotational conformers of HBO exist in the ground state, the *syn*- and *anti*-enols. Moreover, two *syn*-enol isomers exist in a solvent-dependent equilibrium. Of the two isomers, one *syn*-enol has an internal O−H---N bond and one "open" or "solvated" *syn*-enol possesses intermolecular H-bonds with solvent. These *syn*-enols may be differentiated experimentally. Only the "closed" *syn*-enol has an intramolecular O−H---N bond that is required for ESIPT. Therefore, photoexcitation results in efficient ESIPT and strongly red-shifted fluorescence at approximately 500 nm. Excitation of the solvated *syn*- or *anti*-enols results in fluorescence at ∼370 nm, as no ESIPT is possible. The ratio of these two steady-state emission bands may be used to quantitate the concentration of the *syn*-enol relative to the solvated and *anti*-enols. This ratio is large (>20:1) in hexane, demonstrating the almost exclusive presence of the internally H-bonded *syn*-enol, but drops to ∼1:1 and ∼1:6 in methanol and DMSO, respectively, due to the increased H-bonding capacity of these solvents (Figure 2).

The equilibrium between the *syn*- and *anti*-conformers is also solvent dependent. On the basis of the excitation-dependent emission experiments and the time-resolved studies reported in this work, as well as the calculations by Dörr and co-workers,[8] we assign the 318 nm absorption to the *anti*-enol and the 333 nm absorption to the syn isomer. In hexane HBO exists primarily as the *syn*-enol in equilibrium with a small concentration of the *anti*-enol. In MeOH and DMSO, the fluorescence excitation spectra showed a large contribution from the excited states of both solvated *syn*- and *anti*-conformers to the emission at 370 nm. Relative to hexane, DMSO and MeOH each selectively increases the stability of the solvated *syn*-enol of HBO relative to the *anti*-enol. This stabilization may result from specific H-bonding interactions or from polarity effects.

Solvent-Dependent Dynamics of HBO. There are at least three components to HBO tautomerization: enol dynamics; proton-transfer dynamics; keto dynamics. The solvent-dependent dynamics of each component has been characterized. After excitation, the solvated *syn*- and *anti*-enols fluoresce back to their respective ground states, while the internally H-bonded *syn*-enol efficiently tautomerizes to the keto form. The lifetime of the *anti*-enol, ca. 1400 ps, showed no solvent dependence. Since it is expected that an intermolecular H-bond with solvent would contribute to the structural and electronic properties of the *anti*-enol, the solvent independence implies the existence of an intramolecular H-bond. As expected, the solvated *syn*-enol shows a solvent-dependent lifetime. Although the TRF signal was only detectable in methanol and DMSO, the lifetime was twice as long in DMSO compared to methanol. The increased solvent sensitivity of the solvated *syn*-enol is expected, relative to an intramolecularly H-bonded *anti*-enol, due to the intimate involvement of the solvent in this structure. An equilibrium between an unsolvated *anti*-enol and a solvated *syn*-enol is consistent with the observation that the equilibrium is

shifted toward the *syn*-enol with the stronger interacting solvents MeOH and DMSO, relative to hexane.

The closed *syn*-enol, which has an intramolecular H-bond, undergoes efficient proton transfer upon excitation. We observed a 170 fs rise time in the TA measurements, which we assign to the excited-state proton transfer. This rise time is independent of solvent, as well as H to D isotope substitution, consistent with a strongly exothermic proton transfer with weak coupling to solvent degrees of freedom. The isotope independence has often been interpreted as resulting from a barrier-free ESIPT, where the rate is controlled by C−O−H bending vibrations that deliver the proton to the acceptor. However, H to D isotope substitution should decrease the frequency of such bending vibrations by a factor of approximately 1.4, predicting a proton-transfer time constant of ∼240 fs for the heavier isotope, which would be easily detected by the TA experiment. It is therefore possible that the ESIPT occurs adiabatically with a small activation barrier involving HBO vibrations that do not include the H or D atoms, such as torsional motion within the biaryl ring system.

This model of proton transfer is supported by the conclusions of previous studies of related ESIPT systems. For example, Chudoba et al. proposed that ESIPT in 2-(2′-hydroxy-5′-methylphenyl)benzotriazole is modulated by a highly anharmonic in-plane vibration which modulates the separation between proton donor and acceptor atoms and leads the system to a barrierless channel on the excited-state potential.[22] Ab initio study of the ground- and excited-state proton transfer in HBO at the SCF and CIS levels showed that in the course of excited-state nuclear motion the O and N atoms are brought into proximity by in-plane bending.[23] The calculations predicted a decreasing barrier with decreasing O---N distance. In HPMO, a molecule very similar to HBO, two mechanisms were proposed for the proton-transfer dynamics.[14] A direct and barierless proton transfer takes place in ∼100 fs that conserves the system planarity. A second proton transfer route results from a bifurcation of the initially excited wave packet in which some trajectories evolve to the keto state with concomitant rotation of the biaryl bond. Tautomerization along this twisting reaction coordinate involves an energy barrier, as predicted theoretically.[24] For similar systems involving internally H-bonded six-membered rings, Sobolewski et al. predicted barrierless proton-transfer on the basis of CASSCF and CIS electronic-structure calculations.[25]

The lifetime of the excited keto shows a stronger solvent dependence than did the enol isomers described above. The decays varied by a factor of 5 in the different solvents. The lifetime was the shortest in DMSO (57 ps), slightly longer in MeOH (68 ps), and significantly longer in hexane (295 ps). These data are consistent with that reported by Dörr and co-workers, who measured the lifetime of the excited HBO keto state in a large number of solvents.[15] They measured lifetimes that ranged from 69 ps in DMSO to 413 ps in carbon tetrachloride and generally decreased with increasing solvent polarity.

In addition to the minimal number of dynamic processes (enol lifetime, proton transfer rate, and keto lifetime) additional time scale dynamics are reflected in the data. In each TA experiment, one additional component is detected, which has a strong wavelength dependence. With the one-color (333/333 nm) TA this process appears as a 12 ps decay that is a major component of the relaxation; the relative amplitude of the decay is equal to that of the 295 ps decay. The two-color (320/430 nm) TA detects a slower 20 ps decay which is a smaller component of the total decay relative to the 295 ps component (1:9 relative amplitudes). The lower energy probe experiments (333/445 and 338/453 nm) each detect a 560 fs rise time. Unfortunately the uncertainty in the relative amplitudes of the rise times prevents an assessment of their relative contributions.

These decay and rise components may derive from multiple processes whose relative contribution depends on the pump and probe wavelengths. It is possible that the pump pulse excites different ground states or that the probe pulse observes different combinations of ground and excited states. However, it is possible to speculate on the dynamics that might give rise to these data. For example, the 12 ps decays might represent rethermalization of the ground-state molecules disturbed by the probe pulse, which is consistent with the observation of a similar time scale process (7 ps) in MBO. The rise time might correspond to vibrational cooling within the excited keto. Chou et al. reported a 8−10 ps rise time during fluorescence upconversion studies of ESIPT in 10-hydroxybenzo[*h*]quinoline.[26] These authors ascribed this dynamics to vibrational cooling of the excited keto that is initially prepared in a vibrationally hot state after ESIPT, as is also likely with HBO. While 560 fs is considerably faster than 10 ps, it is not unreasonable compared to other vibrational redistribution processes. Zewail et al. observed a decay for HPMO that was fit with time constants of approximately 200 fs and 3 ps and was ascribed to a proton transfer involving initial stretching of the O−H bond followed by torsional motion across a low barrier.[14] It is also possible that the observed dynamics with HBO reflect a complex superposition of several of the above-mentioned processes. Additional experiments, particularly femtosecond fluorescence upconversion, are required to further address these issues.

Conclusions

In the ground state, HBO exists as an equilibrium between the *syn*- and *anti*- enols. The solvent-independent lifetime of the *anti*-enol implies that this rotamer has an internal H-bond between the phenolic hydroxyl group and the benzoxazole oxygen atom. The *syn*-conformer exists in equilibrium between an internally H-bonded enol and the solvated *syn*-enol. The lifetime of the solvated *syn*-enol is longer in the H-bond accepting solvent (DMSO), relative to the H-bond donating solvent (MeOH). The *syn*-enol efficiently undergoes ESIPT upon photoexcitation. The lifetime of the keto proton transfer product is significantly longer in the weakly solvating environment of hexane relative to MeOH and DMSO.

The proton transfer occurs in 170 fs and is independent of solvent or isotope. This implies that the proton transfer occurs over a low barrier in the excited state and involves motions of the molecule that are not strongly sensitive to O−H motion, perhaps intra-aryl ring torsional motion, as is thought to play an important role in related derivatives.

A process which occurred on a 500 fs to 20 ps time scale that is intermediate between the ESIPT and keto lifetimes was also observed. This process may correspond to torsional motion of an alternative ketone product that arises from a second proton-transfer pathway, as has been suggested for the analogous compound HPMO.[14] Additional experiments are currently in progress to further define the molecular nature of this process.

Acknowledgment. We thank Professor Julius Rebek for use of the Spex Fluorolog spectrometer. Funding was provided by the Skaggs Institute for Chemical Biology.

References and Notes

(1) Ormson, S. M.; Brown, R. G. *Prog. React. Kinet.* **1994**, *19*, 45.

(2) Le Gourrierec, D.; Ormson, M. S.; Brown, R. G. *Prog. React. Kinet.* **1994**, *19*, 211.
(3) Ogawa, A. K.; Abou-Zied, O. K.; Tsui, V.; Jimenez, R.; Case, D. A.; Romesberg, F. E. *J. Am. Chem. Soc.* **2000**, *122*, 9917.
(4) Taylor, C. A.; El-Bayoumi, M. A.; Kasha, M. *Proc. Natl. Acad. Sci. U.S.A.* **1969**, *63*, 253.
(5) Abou-Zied, O. K.; Jimenez, R.; Romesberg, F. E. *J. Am. Chem. Soc*. **2001**, *123*, 4613.
(6) Mordzinski, A.; Grabowska, A. *Chem. Phys. Lett.* **1982**, *90*, 122.
(7) Krishnamurthy, M.; Dogra, S. K. *J. Photochem*. **1986**, *32*, 235.
(8) Woolfe, G. J.; Melzig, M.; Schneider, S.; Dörr, F. *J. Chem. Phys*. **1983**, *77*, 213.
(9) Das, K.; Sarkar, N.; Majumdar, D.; Bhattacharyya, K. *Chem. Phys. Lett*. **1992**, *198*, 443.
(10) Mosquera, M.; Penedo, J. C.; Rodríguez, M. C. R.; Rodríguez-Prieto, F. *J. Phys. Chem*. **1996**, *100*, 5398.
(11) Arthen-Engeland, Th.; Bultmann, T.; Ernsting, N. *P. Chem. Phys*. **1992**, *163*, 43.
(12) Laermer, F.; Elsaesser, T.; Kaiser, W. *Chem. Phys. Lett*. **1988**, *148*, 119.
(13) Frey, W.; Laermer, F.; Elsaesser, T. *J. Phys. Chem.* **1991**, *95*, 10391.
(14) Zhong, D.; Douhal, A.; Zewail, A. H. *Proc. Natl. Acad. Sci. U.S.A.* **2000**, *97*, 14056.
(15) Woolfe, G. J.; Melzig, M.; Schneider, S.; Dörr, F. In *Picosecond Phenomena III*; Springer Series in Chemical Physics, Vol. 43; Springer: Berlin, 1982; p 273.
(16) Barbara, P. F.; Brus, L. E.; Rentzepis, P. M. *J. Am. Chem. Soc*. **1980**, *102*, 5631.
(17) Ding, K.; Courtney, S. J.; Flom, S.; Friedrich, D.; Barbara, P. F. *J. Phys. Chem*. **1983**, *87*, 1184.
(18) Itoh, M.; Fujiwara, Y. *J. Am. Chem. Soc*. **1985**, *107*, 1561.
(19) Wilson, K. R.; Yakovlev, V. V. *J. Opt. Soc. Am. B* **1997**, *14*, 444.
(20) Guest, C. R.; Hochstrasser, R. A.; Dupuy, C.; Allen, D. J.; Benkovic, S. J.; Millar, D. P. *Biochemistry*. **1991**, *30*, 8759.
(21) Lochbrunner, S.; Wurzer, A. J.; Riedle, E. *J. Chem. Phys.* **2000**, *112*, 10699.
(22) Chudoba, C.; Riedle, E.; Pfeiffer, M.; Elsaesser, T. *Chem. Phys. Lett.* **1996**, *263*, 622.
(23) Rios, M. A.; Rios, M. C. *J. Phys. Chem.* **1995**, *99*, 12456.
(24) Scheiner, S. *J. Phys. Chem. A* **2000**, *104*, 5898.
(25) Sobolewski, A. L.; Domcke, W. *Phys. Chem. Chem. Phys.* **1999**, *1*, 3065.
(26) Chou, P.-T.; Chen, Y.-C.; Yu, W.-S.; Chou, Y.-H.; Wei, C.-Y.; Cheng, Y.-M. *J. Phys. Chem. A* **2001**, *105*, 1731.